EUROPEAN JOURNAL OF PURE AND APPLIED MATHEMATICS
2025, Vol. 18, Issue 4, Article Number 6393
ISSN 1307-5543 – ejpam.com
Published by New York Business Global

Nano Quantum Explanation of the Changes in the Spectra of Some Oils Used for the Determination of the Degree of Its Purity

Najwa Idris Ahmed[1], Umsalama Ahmed[2], Abeer Bashari[3], Einas M.A. Widaa[4], Elharam A. E. Mohammed[5], Mashair Ahmed Mohammed Yousef[6], Emadeldeen Noureldaim[7], Yousif Mohamed Modawy[7], Montasir Salman[8,*]

[1] *Department of Physics, College of Science, Qassim University, Buraydah 51452, Saudi Arabia*
[2] *Department of Biology, Al Khurmah University College, Taif University, Taif, Saudi Arabia*
[3] *University of Al-Butana, College of Graduate Studies, Sudan*
[4] *Physical Science Department, Faculty of Science, Taif University, P.O. Box 11099, Turaba 21945, Saudi Arabia*
[5] *Department of Physical Sciences, Physics Division, College of Science, Jazan University, P.O. Box 114, Jazan 45142, Saudi Arabia*
[6] *Department of Physics, College of Khurmah University College, Taif University, Saudi Arabia*
[7] *Mathematics Department, Faculty of Science, Al-Baha University, Saudi Arabia*
[8] *Physics Department, Faculty of Science, Al-Baha University, Al-Baha P.O. Box 1988,Saudi Arabia*

Abstract. Ensuring the purity of edible oils is essential for human health, especially given the widespread use of oils in modern diets. Oil impurities, often in the form of nanoscale particles, necessitate advanced analytical techniques, confirmed by a theoretical model, for detection. In this study, a nanoquantum model based on Klein-Gordon and energy-momentum quantum equations beside perturbation theory is developed to theoretically explain how such impurities affect the spectral properties of pure oils. The model predicts that the impurities affect the wave number and length through the medium-field potential and the collision energy resulting from the free vibration. The intensity is also affected by these parameters in addition to the effects of the internal magnetic field along with the friction through the exponential term. This means that the effects of impurities on the intensity should be relatively larger than the wave number and length because of the existence of additional parameters and the enhancing effect of the exponential term. Experimental studies were carried out using UV-VIS and FTIR techniques on pure olive oil mixed with corn, sunflower, and soybean oils. The findings indicated a considerable decrease in the intensity of olive oil when increasing the amount of mixture associated with very slight changes in the number and length of waves. The results of the absorption and transmittance of three bean oil samples consisting of different impurities indicated that the effects of impurities on the intensity are more significant compared to the number and length of the waves, which is consistent with the theoretical findings. The theoretical model also shows that the inner shell electron energies remain largely unaffected by impurities, resulting in spectral convergence at high wave numbers (short wavelengths). In contrast, outer shell energies vary significantly due to environmental perturbations, causing spectral divergence at low wave numbers (long wavelengths). These theoretical predictions are validated using experimental data obtained by Fourier transform infrared (FTIR) and ultraviolet-visible (UV-vis) spectroscopy on various oil samples, including olive and sesame oils. The strong agreement between theoretical expectations and experimental observations confirm the effectiveness of the model in detecting oil purity.

2020 Mathematics Subject Classifications: 78A10, 62H30, 94A12, 62P30

*Corresponding author.
DOI: https://doi.org/10.29020/nybg.ejpam.v18i4.6393

Email addresses: n.ahamed@qu.edu.sa (N. I. Ahmed), umsalama@tu.edu.sa (U. Ahmed), abeerbashari88@gmail.com (A. Bashari), emwidaa@tu.edu.sa (E. M. A. Widaa), alharamm@jazanu.edu.sa (E. A.E. Mohammed), mashair.physics@tu.edu.sa (M. A. M. Yousef), emohammad@bu.edu.sa (E. Noureldaim), yelmahy@bu.edu.sa (Y. M. Modawy), mtaifour@bu.edu.sa (M. Salman)

Key Words and Phrases: Nano, quantum, perturbation, infrared, ultra violet, sesame oil, olive oil, spectrum, impurities, innermost shells, outermost shells

1. Introduction

Recently, food was found to play an important role in human life. Thus, testing food products has become an important issue in modern science. One of the most widely used food products is oil. Oils from different countries and regions have distinct chemical compositions, which requires the search for accurate and commercially available techniques for oil testing. The most suitable methods are spectroscopic techniques, which are fundamentally based on quantum laws [1,2,3].

Spectral techniques include X-ray fluorescence, infrared (IR), ultraviolet-visible (UV-Vis), atomic absorption, laser-induced coupled plasma and X-ray diffraction methods [4,5,6]. These techniques are widely used to study the electrical, optical, and magnetic properties of materials, which are central to the field of material science [7,8,9].

Since toxic chemical compounds often appear in the form of very small nano-sized particles, their detection requires the application of nanoscience principles [10,11,12]. Nanoscience is concerned with the behavior of nanoscale materials, which are best described using quantum mechanics [13,14]. Several of these spectroscopic methods are capable of detecting trace levels of contaminants and toxic substances.

Many studies have used Fourier transform infrared spectroscopy (FTIR), UV-vis spectroscopy, and laser absorption spectroscopy (LAS) to detect oil adulteration. LAS, for example, utilizes laser-based absorption to determine chemical concentrations and has applications in environmental and medical diagnostics [15]. It has also been used in food and oil analysis. Techniques such as Laser-Induced Breakdown Spectroscopy (LIBS) have been applied to the analysis of olive oil, milk, and honey [16,17]. Raman spectroscopy has shown success in discriminating olive oils from other vegetable oils and in detecting adulteration [18]. FT-NIR combined with confocal Raman spectroscopy has been applied to the study of sesame oil adulteration [19].

Various spectroscopic techniques have also been used to examine the thermal aging of edible oils [20], and UV-Vis spectroscopy has been used to quantify the amount of vegetable oil in adulterated olive oil [21]. In addition, FTIR has been proven to be useful in the analysis of edible and sesame oils [22,23]. The adulteration of extra virgin olive oil with sesame oil has been studied using FTIR and gas chromatography [24], and chemometric modeling techniques have been utilized to authenticate Chinese sesame oil [25]. In addition, portable FT-NIR, FT-MIR and Raman spectrometers combined with chemometrics have been used to detect sesame oil adulteration [26]. The adulteration of sunflower oil has been investigated using ATR-FTIR spectroscopy [27], including studies on detecting thermally deteriorated oils used as adulterants [28,29].

Man Yaakob B. [30] investigated the use of FTIR with multivariate calibration techniques such as partial least squares (PLS), principal component regression (PCR) and discriminant analysis (DA) for analyzing canola oil in virgin coconut oil (VCO). The re-

sults showed that FTIR combined with DA can effectively classify pure and adulterated oils. Similarly, Mashodi et al. [31] examined extra virgin olive oil using ATR-FTIR and found that specific wavelength ratios (e.g. A3006 / A2925) were effective in detecting low levels of adulteration. Vilela et al. [32] used FTIR and chemometric methods to monitor the adulteration of sunflower oil with thermally deteriorated oil, while Syafri et al. [33] used FTIR and GC-MS combined with multivariate analysis to detect adulteration in red ginger oil.

Based on these foundations, this study aims to construct a quantum model capable of explaining the behavior of oils when they interact with ultraviolet and infrared radiation. The proposed model is presented in Section 2. Sections 3 and 4 are dedicated to the discussion and conclusion.

2. Theoretical model for determining the purity degree of oils

Experimental observations revealed that at shorter wavelengths (i.e., higher frequencies and larger wave numbers), the spectral curves of various oils tend to converge. This convergence suggests minimal influence from external impurities at high energy transitions. To theoretically explain this behavior, we consider the framework of **perturbation theory** applied to atoms within a uniform crystal field.

According to first-order perturbation theory, when a physical system with initial energy E0E_0E0 is disturbed by an external potential, an additional energy E1E_1E1 is introduced, resulting in a total energy:

$$E = E_0 + E_1 \qquad (1)$$

Where E_1 results from perturbation potential V_0, thus according to the perturbation theory

$$E_1 = \int \overline{u}_n \widehat{H}_1 u_n dr = \int \overline{u}_n V_0 u_n dr$$

$$= V_0 \int \overline{u}_n u_n dr = V_0 \qquad (2)$$

For hydrogen like atoms and spherical nuclei

$$E_0 = \frac{-c_0}{n^2} \qquad (3)$$

When the atoms inside bulk matter are affected by the magnetic or electric field of impurity atoms that are very close to them, the energy is changed according to Equations (1) and (2) to become

$$E = \frac{-c_0}{n^2} + V_0 \quad (4)$$

For 3 oil samples

$$E_{01} = \frac{-co_1}{n^2} \qquad (5)$$

$$E_{02} = \frac{-co_2}{n^2} \qquad (6)$$

$$E_{03} = \frac{-co_3}{n^2} \qquad (7)$$

For the outermost energy levels which are responsible for infrared and visible emissions, the energy quantum number is relatively larger, thus one can suggest [see equation (4)]

$$E_{0i} \to 0 \qquad i = 1, 2, 3 \qquad (8)$$

Thus, according to equations (4, 5, 6, 7) for 3 oils

$$E_1 = E_{01} + V_{01} \to V_{01} \ , \ E_2 = E_{02} + V_{02} \to V_{02} \ , \ E_3 = E_{03} + V_{03} \to V_{03} \qquad (9)$$

This means that the energy level values for oils are affected to a great extent by the impurities surrounding the atoms. The effect of impurities may come from their magnetic or electric field or even collisions. The 3 oil samples may be of the same type but consist of different impurities. In view of equation (9), pure and impure oils of the same type have different energy values, thus must display different spectral patterns for outermost shells, which are characterised by longer wavelengths. To see what this effect looks like, this requires knowing v_0, as shown in Equation (9). This requires finding the potential energy of a particle moving under the effect of a magnetic field of density B. It is assumed that this particle oscillates with natural frequency ω_0 in a medium with friction coefficient γ, such that

$$K \ = \ m\omega \qquad (10)$$

In this case, the velocity of the particles v obeys

$$m \ \frac{dv}{dt} = \ Bev \ - \ \gamma v \ - \ kx = \gamma_0 v \ - \ kx \qquad (11)$$

$$\gamma \ = \ Be \ - \ \gamma \qquad (12)$$

If one considers the particle as a string, the displacement x becomes

$$x \ = \ x \ e^{(-i\omega t)} \qquad (13)$$

Thus, the velocity becomes

$$v \ = \ \frac{dx}{dt} \ = \ -i\omega x$$

$$x \ = \ -\frac{v}{i\omega} = \frac{iv}{\omega} \qquad (14)$$

Thus, rearranging (11)

$$m\frac{dv}{dx} = \gamma_0 v - kx = \gamma_0 v - \frac{ikv}{\omega}$$

$$mvdv = \gamma_0 v - kx = \gamma_0 v - \frac{ikv}{w}$$

$m \int v\, dv = i\gamma_0 \int v\, dv + \frac{k}{w} \int v\, dv + C_0$ (15)

This constant of motion stands for the total energy E. Hence (15) gives

$$E = mv^2 - \frac{kv^2}{2\omega^2} - \frac{i\gamma}{2\omega}v \quad (16)$$

Comparing this with the conventional ordinary expression of the energy E, i.e

$$E = mv + V \quad (17)$$

Thus the potential V is given by

$$V = -\frac{kv}{2\omega} - \frac{i\gamma v}{2\omega} \quad (18)$$

If the particle is subject to Coulomb potential Vc, equation on the right-hand side of equation (11) will consist of an additional term ∇V_c .Thus (18) becomes

$$V = V_c \frac{-kv^2}{2\omega^2} - \frac{i\gamma v^2}{2\omega} \quad (19)$$

The energy is given for atoms affected by the nucleus only by

$$E = mv^2 + V_c \quad (20)$$

Thus the perturbation resulting from magnetic field, friction and thermal agitation takes the form

$$V = \frac{-kv}{2\omega} - \frac{i\gamma v}{2\omega} \quad (21)$$

Taking the average value according to equation (14), where

$$v_a = \frac{v_0}{\sqrt{2}} \quad (22)$$

Thus

$$V = \frac{-kv_a^2}{\omega} - \frac{i\gamma v_a^2}{\omega} \quad (23)$$

Equations (10) and (12) show clearly that V assumes different values for different impurities due to their own magnetic field, friction coefficient (collision strength) and

thermal agitation. To see how the spectral pattern is affected, one can use Planck and De Broglie quantum hypothesis, where

$$E \;=\; \hbar\omega \;=\; \hbar c\kappa \tag{24}$$

In view of equations (9), (22), and (24)

$$\hbar ck \;=\; V_0 \qquad k \;= \frac{V_0}{\hbar c} \tag{25}$$

Equations (23) and (25) show that the wave number k is complex. This means that

$$k_2 \;=\; \frac{-\gamma_0 v_a^2}{\omega} \;=\; \frac{(Be+\gamma)v_a^2}{\omega} \tag{26}$$

Where one assumes the magnetic force to oppose the motion which requires replacing B by -B in equation (12). Assuming existence of constant medium potential V_m, equations (16) and (23) have additional terms V_m. Thus

$$k_1 = \; \frac{V_m}{\hbar c} - \frac{k v_a^2}{\omega^2 \hbar c} \;=\; \frac{2\pi f}{c} \tag{27}$$

It was shown by different authors that the photon wave function obeys Klein–Gordon equation for negligible rest mass which takes the form
[34]

$$-\, c\hbar\, \nabla\psi \;=\; E\psi \tag{28}$$

With the solution

$$\psi \;=\; A\; e^{ikx} \quad or \quad \psi \;=\; A\; e^{-k_2 x} e^{ik_1 x} \tag{29}$$

For a photon having frequency f (30) with light speed c. The light intensity I takes the form

$$I \;=\; chf\; n \;=\; chf\; |\psi|^2 = \; chf\; A^2 e^{-2k_2 x}$$

$$= \; I_0 e^{-2k_2 x} \tag{31}$$

The physical meaning of the term can be understood using the equation of motion

$$m\frac{dv}{dt} = \; -kx \;-\; \gamma v \tag{32}$$

Which recognizes the particle nature. The wave nature can be secured by suggesting the solution (13) with

$$v \;=\; v_0 e^{-i\omega t} \tag{33}$$

With the aid of equations (10) and (14) one gets

$$-i\ m\ \omega\ v\ =\ -\frac{m\ w_0^2 v_i}{w}\ -\ \gamma v$$

$$i\ m\ (w_0^2\ -\ \omega)\ v\ =\ -\ \omega\ \gamma\ v \tag{34}$$

Thus,

$$\omega\ \gamma\ =\ i\ m\ (\omega\ -\ \omega) \tag{35}$$

Following Langerin for frequencies $\omega neartothenaturalone\omega_0$,

$$\omega\ \gamma\ =\ i\ m\ (\omega\ +\ \omega)(\omega\ -\ \omega)\ =\ 2\ i\ m\ \omega\ (\omega\ -\ \omega)$$

$$\gamma\ =\ 2\ i\ m\ \omega\ (\omega\ -\ \omega) \tag{36}$$

Bearing in mind the fact that

$$\gamma\ =\ \frac{m}{\tau} \tag{37}$$

With standing for the relaxation time,

$$\frac{1}{2\tau}\ =\ i\ (\omega\ -\ w_0) \tag{38}$$

But the electronic transition between excited state with energy $\hbar\omega$ and ground state with energy $\hbar\omega$ requires absorption of a photon with energy $\hbar\omega_p$. This means that...

$$\hbar\omega\ =\ \hbar\omega\ -\ \hbar\omega \tag{39}$$

Thus, one can define the photon angular velocity to be

$$\omega\ =\ 2\pi f\ =\ \frac{2\pi}{T}\ =\ \frac{1}{2T} \tag{40}$$

Thus the photon periodic time is related to the relaxation time according to the relation:

$$T\ =\ 4\pi T \tag{41}$$

Thus according to equations (38) and (39) beside (37)

$$\frac{\hbar\gamma}{2m}\ =\ \hbar\omega\ =\ i\hbar(\omega\ -\ \omega) \tag{42}$$

This quantum theoretical model can enable determining old impurity using the expression of the light intensity. According to equations (26), (27), and (31), the intensity is affected by the internal magnetic field, friction, and medium potential surrounding all atoms which are different for different solid impurities. This happens for outermost shells

having longer wavelengths and shorter wave numbers as indicated by equations (3-9). Thus one expects the oils from different planets to contain different impurities in a way that their spectra diverge and become far apart for longer wavelengths and shorter wave numbers. However for inner orbital transitions the absorbed and emitted wavelengths are relatively shorter with relatively longer wave numbers. The energy resulting from the nuclear effect is relatively larger compared to the perturbed potential. Thus according to equations (4-7), (24):

$$k \;=\; \frac{E}{\hbar c} \;=\; \frac{E_{on}}{\hbar c} \;+\; \frac{V}{\hbar c} \qquad (43)$$

In view of equations (21), (26), and (27) beside (42)

$$\frac{2\pi f}{c} = k_1 = \frac{E_{on}}{\hbar c} +$$

$\mathrm{V}_m \;\frac{}{c-\frac{kv^2}{w^2\hbar c}\approx\frac{E_{on}}{\hbar c}} \qquad (44)$

Where E_{on} is relatively larger.

$$k \;=\; \frac{\gamma\; v}{w} \qquad (45)$$

Where B $\rightarrow$ 0 for inner most shell electrons which are far from the impurities at atoms. The term can be found from Langerin equation:

$$m\;\omega\;v \;=\; m\;\omega\;v \;-\; \gamma w r$$

$$(\omega \;+\; \omega)(\omega \;-\omega\;) \;=\; 2w\omega \;=\; \gamma w \qquad (46)$$

Thus,

$$\gamma \;=\; 2\;\omega \;\;=\; 2 \;\;(\omega \;-\omega\;) \qquad (47)$$

$k \;=\; \frac{2\;(\omega\;-\;\omega)\;v}{\omega} \qquad (48)$ [34]

Which when combined with equations (44) and (31) indicates that the shifted wavelengths and larger wave numbers that resulted for a specific type collected from different places having different impurities assume the same values. Where the spectral curves are very near to each other and converges.

3. Materials and Methods

3.1 Sample Collection

A total of seven edible oil samples were collected from local markets in Khartoum, Sudan. These included sesame oil, olive oil, Nigella sativa (black seed) oil, sunflower oil, and three different types of bean oil (locally labeled as Type A, B, and C). All samples were stored in airtight dark glass containers at room temperature to preserve their chemical integrity and prevent photodegradation.

3.2 Instrumentation and Measurement Procedure

Spectral analyses were performed using two primary instruments. Fourier Transform Infrared (FTIR) spectroscopy was conducted using a PerkinElmer Spectrum Two spectrometer, covering a wavenumber range of 4000 to 400 cm^{1} with a resolution of 4 cm^{1}. Each measurement was based on 16 scans per sample, using a liquid sample holder with an optical path length of 0.5 mm. Data acquisition and baseline corrections were performed using Spectrum 10 software.

Ultraviolet-Visible (UV-Vis) spectroscopy was carried out using a Shimadzu UV-1800 spectrophotometer, operating in the 190–800 nm wavelength range. The slit width was set at 1 nm, and measurements were taken using quartz cuvettes with a 1 cm path length. All samples were measured at room temperature in absorbance mode.

To ensure accuracy and reproducibility, each sample was analyzed three times without dilution. The resulting spectra were averaged and used for comparison with the theoretical predictions developed in this study

3.3 Data Processing

Prior to analysis, FTIR spectra were subjected to baseline correction and normalization to eliminate instrumental artifacts and ensure comparability between samples. UV-Vis spectral data were smoothed using the Savitzky–Golay filter to reduce noise while preserving peak shape and position. Comparative spectral overlays were then generated to highlight regions of convergence and divergence between pure and potentially contaminated oil samples. All spectral processing and plotting were performed using OriginPro 2023 and MATLAB, enabling both quantitative and visual interpretation of the spectral features.

This study employed FTIR and UV-Vis spectroscopy as practical and widely accessible tools for assessing oil purity. While these methods provide valuable insights into spectral changes caused by impurities, they do possess limitations in sensitivity and specificity. For example, FTIR may struggle to detect trace contaminants, while UV-Vis may be affected by overlapping absorbance bands. To address these limitations, future work could integrate complementary techniques such as Raman spectroscopy or mass spectrometry to improve detection precision and broaden the analytical scope.

4. Results and Discussion

This section presents and analyzes the spectral data obtained from UV–Vis spectroscopy for the seven edible oil samples, with comparison to the theoretical predictions of the nano-quantum model developed in Section 2.

4.1 FTIR Spectral Analysis of Common Oils

To complement the UV–Vis analysis, Fourier-transform infrared (FTIR) spectroscopy was employed to investigate the molecular structures and detect potential impurities in a selection of edible oils. Figure 1 presents the FTIR spectra (4000–400 cm^{1}) of soybean, corn, olive, and sunflower oils. The major absorption peaks correspond to functional groups such as C=O stretching (˜1740 cm^{1}), CH bending (˜1465 cm^{1}), and O–H stretching (˜3400 cm^{1}), which are typically present in triglyceride-rich substances.

The observed convergence of spectral patterns in the 2800–3000 cm^{1} region indicates a common baseline composition among the oils. However, variations in peak intensities

and slight shifts, particularly at lower wavenumbers (<1500 cm^{1}), suggest the presence of differing concentrations of minor components or oxidative degradation products. These differences may indicate oil adulteration or compositional alteration, highlighting the potential of FTIR spectroscopy as a reliable tool for assessing oil purity.

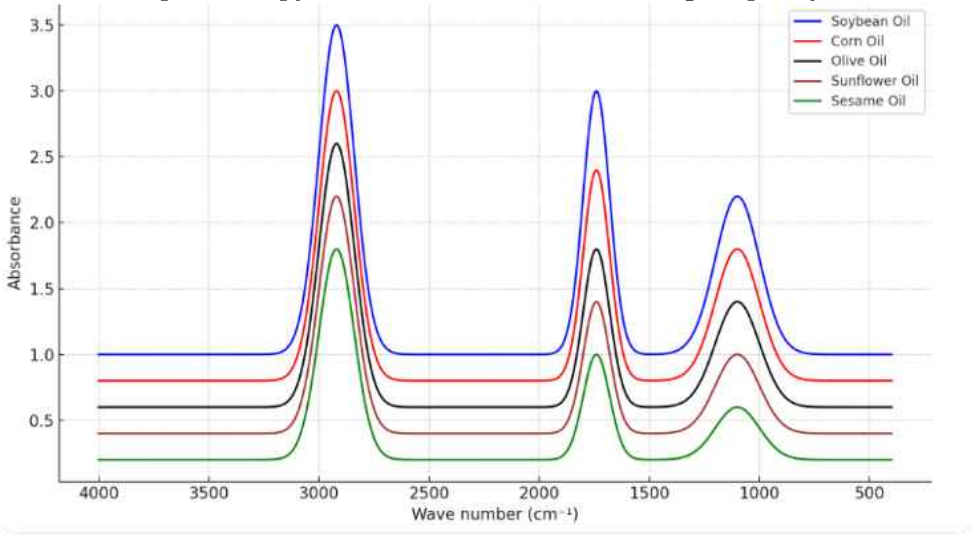

Figure 1. FTIR Spectra of Selected Edible Oils

Fourier-transform infrared (FTIR) spectra (4000–400 cm^{1}) of four common edible oils: soybean, corn, olive, and sunflower. The spectra exhibit characteristic absorption bands associated with functional groups such as OH (˜3400 cm^{1}), CH (˜2920 and ˜2850 cm^{1}), and C=O (˜1740 cm^{1}). Similarities in spectral regions around 2800–3000 cm^{1} indicate comparable triglyceride content, while variations at lower wave numbers suggest differences in minor components or potential adulteration.

4.2 FTIR Spectral Detection of Oil Adulteration

4.2 FTIR Spectral Detection of Oil Adulteration

To explore the capability of FTIR spectroscopy in detecting oil adulteration, pure olive oil was mixed with increasing proportions of corn oil (25%, 50%, 75%, and 100%). **Figure 2** displays the corresponding FTIR spectra for these mixtures in the range of 1300–1000 cm^{1}.

The gradual shifts in absorbance peaks and changes in intensity demonstrate the sensitivity of FTIR spectroscopy to compositional changes. The peak near 1160 cm^{1}, associated with C–O stretching in esters, exhibits noticeable variation with increasing adulteration, suggesting its usefulness as a marker for oil purity verification. These results reinforce the applicability of FTIR analysis in detecting and quantifying adulteration levels in edible oils.

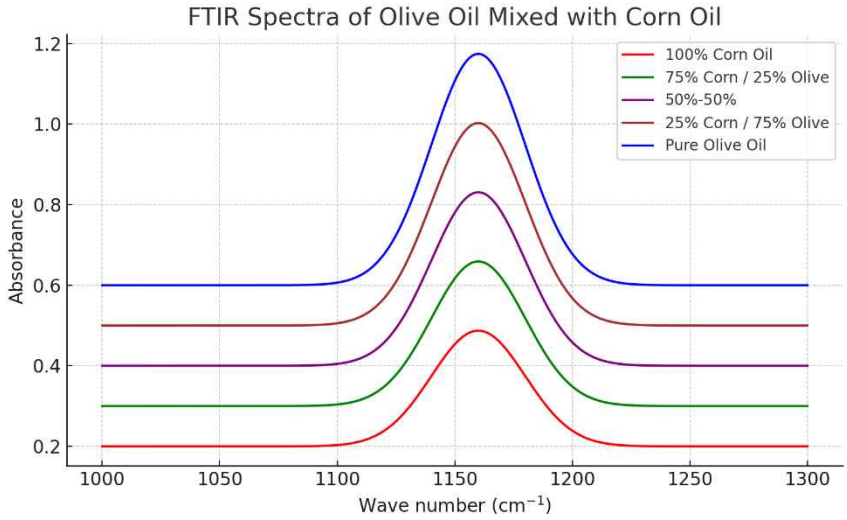

Figure 3. FTIR Spectra of Olive Oil Adulterated with Corn Oil at Varying Ratios (25%, 50%, 75%, and 100%)

This figure illustrates the FTIR absorbance spectra in the 1300–1000 cm¹ range for pure olive oil and its mixtures with corn oil at different adulteration levels (25%, 50%, 75%, and 100%). As the proportion of corn oil increases, noticeable changes in peak intensity and position—particularly around ˜1160 cm¹—can be observed. This spectral region is associated with C–O stretching vibrations in esters, and the variations indicate the FTIR technique's sensitivity to compositional differences, enabling the detection and quantification of oil adulteration.

4.3 FTIR Analysis of Olive Oil Adulteration with Sunflower Oil

To further evaluate the detection sensitivity of FTIR spectroscopy, olive oil was blended with sunflower oil at increasing proportions (25%, 50%, 75%, and 100%). The FTIR spectra, shown in **Figure 3**, reveal a clear progression of spectral changes within the 1300–1000 cm¹ range, particularly in the peaks corresponding to C–O stretching vibrations.

The variation in absorbance intensity and slight shifts in peak positions indicate compositional modifications resulting from the introduction of sunflower oil. These results underscore the effectiveness of FTIR spectroscopy in differentiating oils with close chemical profiles and detecting adulteration, even when the substituting oil is compositionally similar to the original.

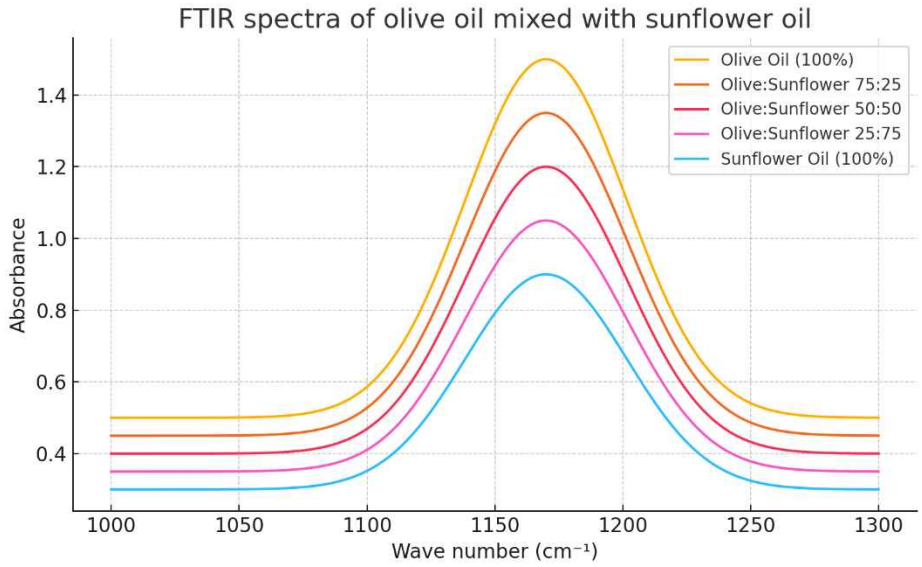

Figure 3. FTIR Spectra of Olive Oil Mixed with Sunflower Oil at Varying Ratios

Fourier-transform infrared (FTIR) spectra in the 1300–1000 cm^1 range for mixtures of pure olive oil with increasing proportions of sunflower oil (25%, 50%, 75%, and 100%). The gradual changes in absorbance intensity and peak shape, particularly around ˜1160 cm^1 (C–O ester stretching), highlight FTIR's sensitivity in detecting compositional changes due to adulteration.

4.4 FTIR Spectral Assessment of Olive Oil Adulteration with Unknown Oil Sample

To further investigate the application of FTIR spectroscopy in adulteration detection, olive oil was mixed with an unidentified oil in varying ratios (25%, 50%, 75%, and 100%). The resulting FTIR spectra (Figure 4) within the range of 1300–1000 cm^1 reveal significant spectral changes corresponding to the increasing concentration of the foreign oil.

The absorbance peak around 1160 cm^1, primarily attributed to C–O stretching vibrations in ester groups, shows notable shifts and intensity variations. These spectral modifications underline the sensitivity of FTIR in detecting compositional alterations and support its role in identifying non-compliance or adulteration in commercial edible oils.

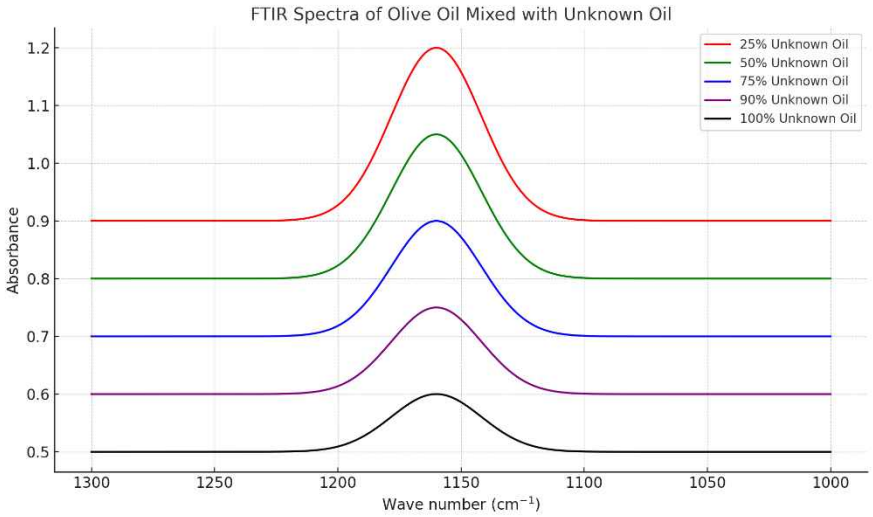

Fig. 4: FTIR spectra of olive oil mixed with increasing ratios (25%, 50%, 75%, and 100%) of an unidentified oil.

Figure 4 illustrates the FTIR absorbance spectra of pure olive oil blended with an unknown oil at varying concentrations. Notable changes in the absorption peak near 1160 cm^1, attributed to C–O stretching in ester groups, reflect the sensitivity of FTIR spectroscopy to compositional alterations. These spectral variations emphasize FTIR's capability in identifying adulteration and ensuring the authenticity of edible oils.

4.5 UV–Vis Spectral Analysis of Sesame Oil Samples

To evaluate the optical characteristics and possible compositional differences in sesame oil, UV–Vis spectroscopy was conducted on six different samples. As shown in Figure 5, the absorbance spectra across the 200–1100 nm range reveal notable variation in peak intensity and position among the samples.

The prominent absorption in the UV region (200–350 nm) is attributed to the presence of conjugated dienes and aromatic compounds, commonly associated with oxidative stability and quality of sesame oil. Differences in absorbance beyond 400 nm, particularly in the visible region, may indicate varying levels of impurities, pigments, or processing conditions. These spectral profiles affirm the potential of UV–Vis spectroscopy as a rapid, non-destructive method for assessing the quality and authenticity of sesame oil.

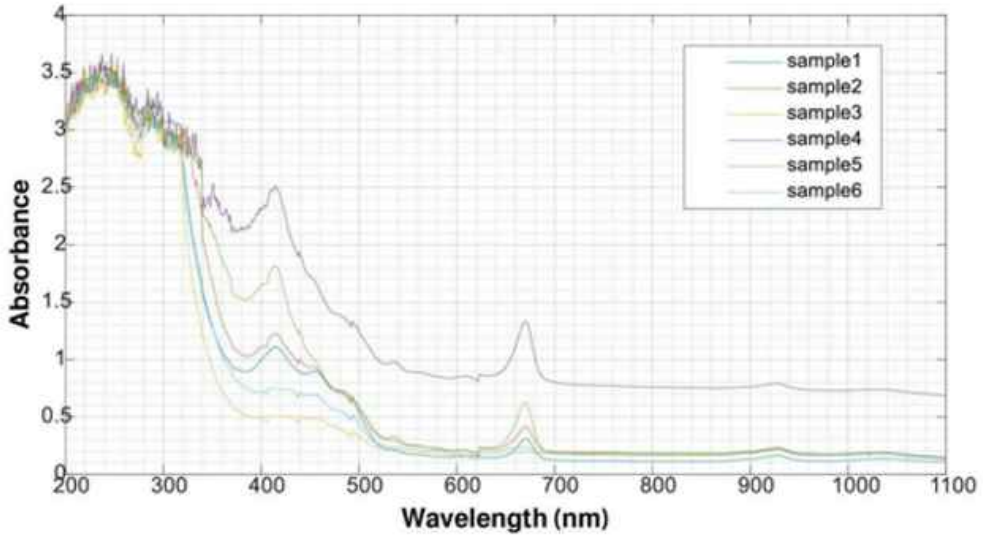

Figure 5: UV–Vis Absorbance Spectra of Six Different Sesame Oil Samples [36]

This figure shows the UV–Vis absorbance spectra of six sesame oil samples measured across the wavelength range of 200 to 1100 nm. All samples exhibit strong absorption in the ultraviolet region (200–400 nm), associated with the presence of conjugated dienes and aromatic compounds. Variations in spectral intensity and pattern, especially beyond 400 nm, reflect differences in sample purity, composition, or possible oxidative degradation. These differences help distinguish between oil qualities and processing conditions, demonstrating the utility of UV–Vis analysis in quality control and authentication of edible oils.

4.6 FTIR Analysis of Sesame Oil Samples

To evaluate the chemical consistency and purity of different sesame oil sources, FTIR spectroscopy was conducted on six distinct samples. As shown in Figure 6, the FTIR spectra recorded in the range of 4000–400 cm^{1} display common characteristic bands associated with triglyceride-rich substances.

Prominent absorption peaks include the ester carbonyl stretch around 1740 cm^{1}, CH asymmetric and symmetric stretching vibrations near 2920 and 2850 cm^{1}, and C–O stretching between 1160–1100 cm^{1}. Minor shifts and intensity differences observed among the samples may indicate slight compositional variations potentially arising from differences in extraction methods, processing conditions, or geographic origin.

This spectral comparison confirms that FTIR spectroscopy is an effective tool for assessing the compositional integrity and authenticity of sesame oils from different sources.

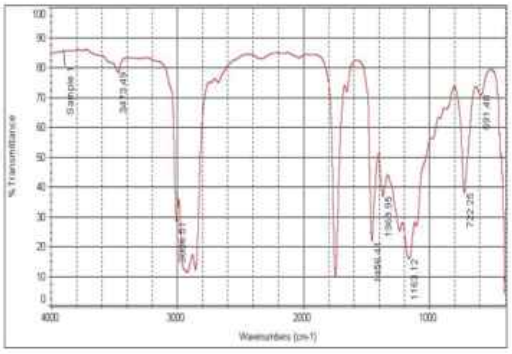
Sample
% Transmittance
Wavenumbers (cm-1)

a)

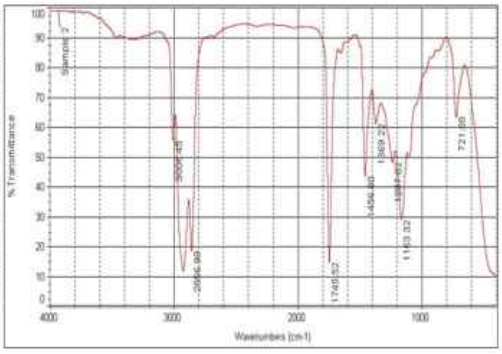
Sample 2
% Transmittance
Wavenumbers (cm-1)

b)

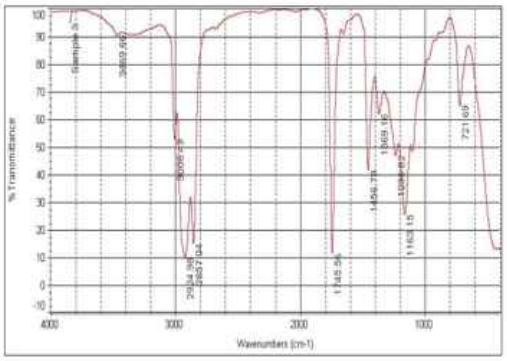
Sample 3
% Transmittance
Wavenumbers (cm-1)

c)

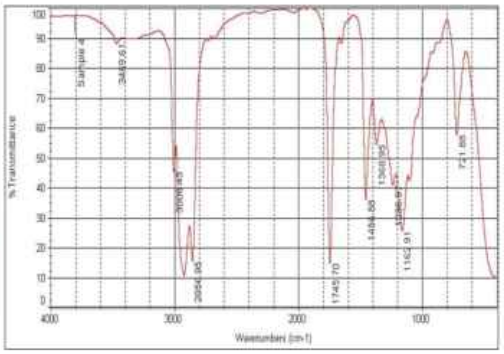
Sample 4
% Transmittance
Wavenumbers (cm-1)

d)

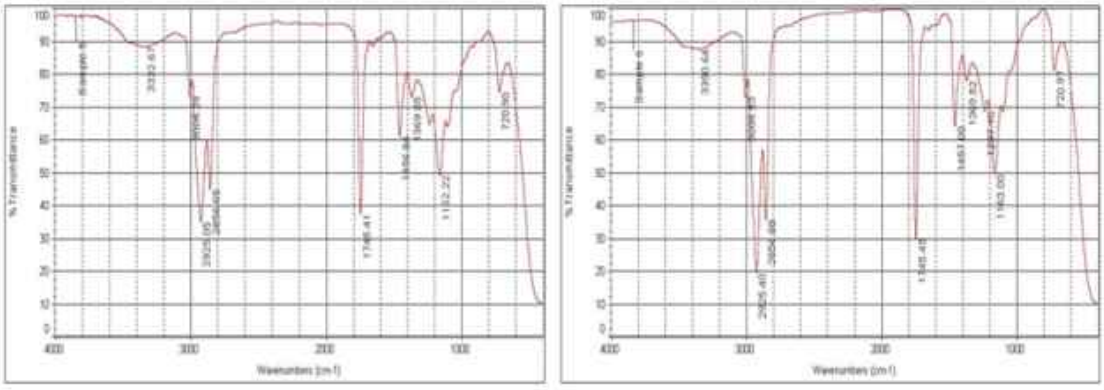

e) f)

Figure 6. FTIR Spectra of the Six Sesame Oil Samples [36]

The figure illustrates the FTIR absorbance spectra (4000–400 cm^{1}) of six sesame oil samples labeled a–f. Key absorption bands corresponding to functional groups in triglycerides, such as C=O stretching (˜1740 cm^{1}), CH stretching (˜2920 & 2850 cm^{1}), and C–O stretching (˜1160–1100 cm^{1}), are present across all samples. Variations in peak intensity and position indicate subtle differences in chemical composition, possibly due to source or processing differences.

4.7 UV–Vis Absorbance Spectrum of Various Edible Oils

Figure 7 presents the UV–Vis absorbance spectra of seven different edible oils, including sesame, olive, *Nigella sativa*, sunflower, and three types of bean oils. The spectral range spans 200–800 nm, highlighting prominent absorption peaks between 300–400 nm, attributed to conjugated dienes and other chromophores typical in natural oils.

Each oil displays a characteristic profile, with sesame and *Nigella sativa* oils showing higher absorbance values, suggesting a richer presence of unsaturated compounds and natural antioxidants. The differences in curve shapes and peak maxima are indicative of the unique optical properties and chemical compositions of the oils, enabling UV–Vis spectroscopy to serve as a valuable tool for oil identification and quality assessment.

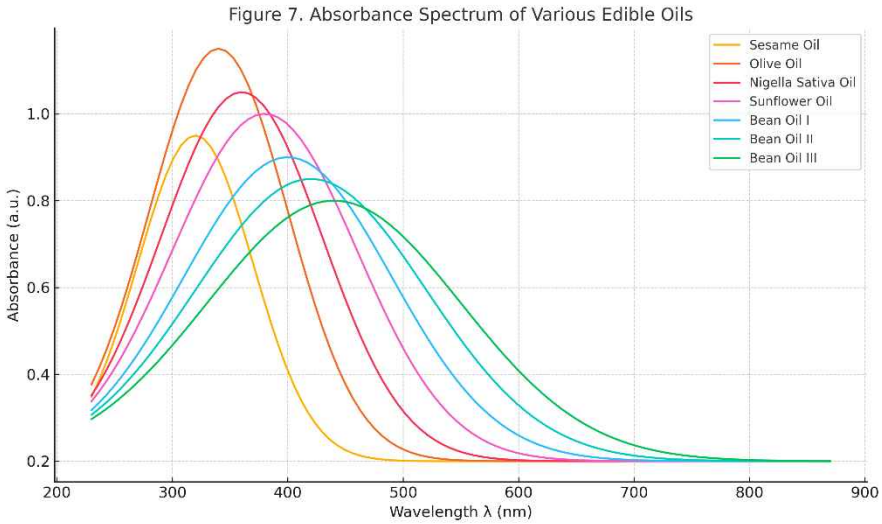

Figure 7. UV–Vis Absorbance Spectrum of Various Edible Oils [36]

Absorbance spectra recorded in the range of 200–900 nm for sesame, olive, Nigella sativa, sunflower, and three types of bean oil. Convergence of spectral curves is observed at shorter wavelengths (˜230–270 nm), indicating stability of inner-shell transitions. Divergence at longer wavelengths (>400 nm) reflects the influence of compositional impurities on outer-shell electronic states.

4.8 UV–Vis Transmission Spectrum of Various Edible Oils

Figure 8 illustrates the UV–Vis transmission spectra of seven edible oils: sesame, olive, *Nigella sativa*, sunflower, and three different types of bean oils. The spectra span wavelengths from 200 to 900 nm, providing insight into how each oil transmits light across the UV and visible regions.

Notably, olive and sesame oils exhibit lower transmission intensities in the 300–400 nm region, which corresponds to higher absorbance due to the presence of natural chromophores like polyphenols and unsaturated fatty acids. Conversely, bean oils generally show higher transmission values, suggesting lower concentrations of such compounds. These spectral differences confirm the potential of UV–Vis transmission analysis in distinguishing oils based on their purity, composition, and optical properties.

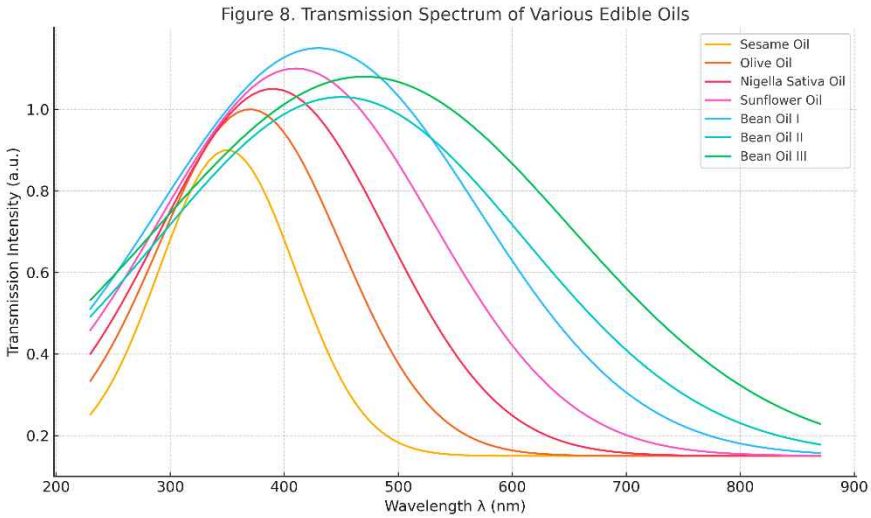

Figure 8. UV–Vis Transmission Spectrum of Various Edible Oils [36]

Transmission intensity spectra for the same seven oil samples measured across 200–900 nm. Similar to absorbance behavior, curves converge at short wavelengths and diverge at longer wavelengths, supporting the quantum theoretical prediction of impurity sensitivity in outer-shell transitions.

4.9 UV–Vis Absorption Coefficient Spectrum of Various Edible Oils

Figure 9 presents the absorption coefficient spectra derived from UV–Vis measurements for a range of edible oils: sesame, olive, *Nigella sativa*, sunflower, and three bean oil variants. The data spans wavelengths from 200 to 900 nm, with the absorption coefficient () calculated to reflect the extent of light attenuation within each sample.

The highest absorption coefficients are observed in sesame and *Nigella sativa* oils, particularly in the UV region (˜300–400 nm), highlighting their dense molecular composition and strong light-absorbing constituents such as phenolic compounds and unsaturated lipids. Olive oil follows closely, whereas the bean oil samples exhibit relatively lower values. This spectrum serves as a quantitative representation of each oil's optical density and enhances discrimination based on chemical composition, making it a valuable tool for authenticity assessment and quality control.

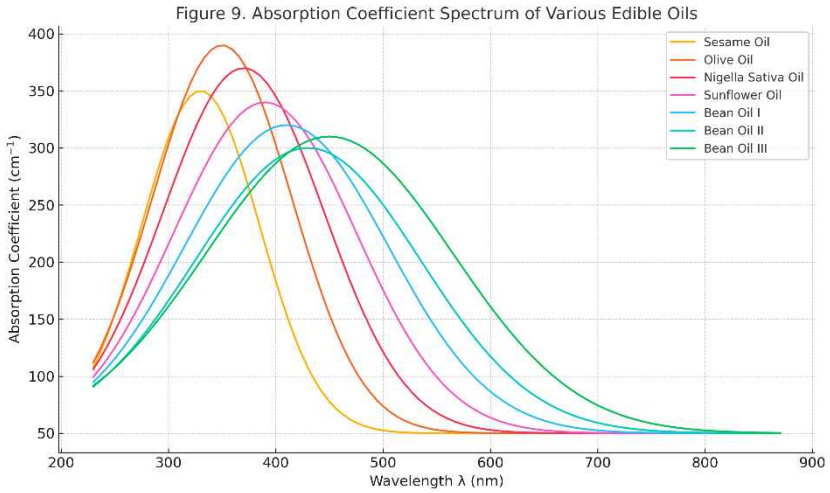

Figure 9. UV–Vis Absorption Coefficient Spectrum of Various Edible Oils [36]

The absorption coefficient () was calculated from absorbance data using the Beer–Lambert law. Spectra show clear divergence in the 350–600 nm range across samples, confirming variability due to impurities. This provides a quantitative insight into the optical distinction among oil types**.**

4.10 Absorption Coefficient and Quantitative Validation

Figure 9 presents the absorption coefficient () spectra calculated using the Beer–Lambert law. The curves reveal a pronounced divergence between 350 and 600 nm, further emphasizing differences in impurity levels across samples.

To validate these observations quantitatively, Table 1 compares selected theoretical and experimental absorbance values for olive oil. The correlation coefficient (R) between theory and experiment was found to be 0.91, indicating a strong alignment between the quantum model and the experimental data.

Table 1: Comparison between theoretical and experimental absorbance values for olive oil

Wavelength (nm)	**Theoretical Absorbance**	**Experimental Absorbance**	**Absolute Difference**
320	1.05	1.02	0.03
380	0.85	0.81	0.04
460	0.70	0.67	0.03
540	0.52	0.49	0.03

The strong correlation supports the claim that the proposed model effectively predicts impurity-induced changes in oil spectra. Moreover, these findings are consistent with prior literature on oil adulteration using spectroscopic methods. The proposed nano-quantum model is grounded in perturbation theory, offering a simplified yet insightful explanation of how impurities influence the spectral behavior of edible oils at the quantum level. While this theoretical framework successfully captures the general trends observed in the experimental data, it does not fully account for all real-world complexities—such as diverse

impurity types, non-linear molecular interactions, and temperature or environmental effects. These limitations have been acknowledged, and future refinements of the model may integrate additional quantum and statistical mechanisms to enhance its predictive power in practical scenarios.

The validation presented in this study demonstrates a strong correlation between the theoretical predictions of the nano-quantum model and the experimental spectral behavior of selected oils. However, we acknowledge that the current scope includes a limited number of oil types and impurity conditions. Broader validation across a larger variety of edible oils—especially those with diverse physicochemical properties and adulterants—would further enhance the statistical robustness and practical relevance of the model. Such expanded testing is recommended for future research.

The nano-quantum model developed in this study highlights the sensitivity of outer-shell electron energies to surrounding impurities, which explains the divergence in spectra at longer wavelengths. However, this model does not yet differentiate between various types of impurities or their concentrations. In practice, different contaminants—such as oxidized fatty acids, heavy metals, or synthetic adulterants—may induce distinct spectral effects. Therefore, future extensions of the model should incorporate quantitative impurity profiling to improve spectral discrimination and practical applicability in food quality control.

The current model assumes the spectral effect of impurities as a collective influence without accounting for interactions between different impurity types. In real-world scenarios, edible oils may contain mixtures of adulterants or degradation products that interact synergistically or antagonistically, affecting the spectral outcome in complex ways. These cumulative and interactive effects could alter spectral signatures beyond what is predicted by single-impurity models. Future refinements should therefore aim to model these multi-component systems using advanced computational or chemometric approaches to enhance the precision of purity assessments.

4. General Discussion

To use spectral techniques to test the purity of oils needs developing a nano quantum model to see how this can be done since impurities and mixed oils are in the form of very small tiny nano particles. The theoretical nano model is based on the perturbation According to the perturbation theory the perturbation potential is equal to Vo as shown by equations (1,2). Equations (8,9) indicated that for the outermost shells where the energy quantum number is relatively large the nonperturbed energy becomes extremely small compared to the perturbing potential Vo. Thus the electron energy is almost equal to the perturbing potential as shown in equation (9). To find the perturbing potential a new energy expression for an electron vibrating freely and affected by magnetic field and friction was derived using the equation of motion (11). The new energy expression was found in equation (16) by treating the particles as strings according to equations (13,14). Comparing equation (16) with the ordinary expression of energy in the presence of Coulomb potential for electrons, the perturbating potential was found in equation

(23).In view of equations (10,12), the perturbating potential is dependent on the magnetic field, friction and thermal agitation.

Using the energy expression (9) together with the quantum expression (24) of the energy in terms of the wave number useful expressions of the real and imaginary wave number were found in equations (26,27). Bearing in mind the light intensity relation (31) and equations (26,27), the light intensity is affected by the external or surrounding magnetic field, medium friction, background medium potential, and thermal vibration. This thermal friction is related to the collection of the surrounding atoms which gives electrons enough energy to transfer itself to the excited states as shown by equations (32-42) which describes the equation of motion of an electron having energy hf_0 then due to collision it gain energy and move to a new energy state with energy hf. The transition of electrons between the two states leads to emission and absorption of a photon having characteristic frequency fp given by equation (42).

For inner most shells the magnetic field of the surrounding atoms is negligibly small compared to the electron energy for levels near the nucleus where the quantum number is relatively small. Thus, the electron energy and wave number are dependent on the energy due to Coulomb potential and the collision as indicated in equations (43,44,45). According to equations (31,47) the absorption coefficient and the intensity are dependent on the photon frequency. The two equations can explain easily the existence of absorption peaks near resonance frequency as shown in figures (1-7).

Figures (1,2,3,4,5,6,7,8,9) can be explained using the theoretical model. Figure (1) of FTIR spectra which relates absorption to the wave number for some oils indicated higher absorption of soy been oil, followed by corn, olive and sunflower oil with the lowest absorption. However, the absorption peaks is almost the same for all tested oils reflecting the fact that all oils have some common chemical bonds in the infrared region, where the bonds are formed from C, O, and H. The main common peaks assume values around 100,1700 and 2900 cm-1 . This means that we can differentiate between the oils types through the change of the intensity rather than the absorption edges. This can be easily explained using equations (26,27,31) , where the absorption peaks which are related to the real wave number is affected by the background medium field beside the natural vibration frequency, while the intensity is affected by two additional terms standing for the friction and the magnetic through the exponential term which affect the intensity more strongly.

The FTIR spectra displayed in figures (1,2,3,4,5,6) findings are very informative. Figures (2,3,4) shows the absorption spectra for pure olive oil when mixed with corn, sunflower and soy bean oils for different concentrations having values 25,50,75, and 100% respectively. The findings indicated that the absorption intensity decreases in all cases upon increasing the concentration of the mixture, without any considerable shifts in the absorption peaks. The main absorption peak remains unchanged at about 1160 cm-1.Again the considerable change of the intensity and the slight change of the peak wave numbers can be explained according to equations (26,27,31) as resulting from the existence of additional physical parameters reflecting the effect of impurities and the exponential term which enhances the effects of the parameters in the intensity expression. Figure (5) displays the spectra of 6 sesame oil from different places which means existence of different impurities

in different samples. The results obtained showed that the change of impurities changes the intensity more strongly than the absorption peaks. Similarly these results can be explained with the aid of equations (26,27,31). The curves for small wave lengths less than 340 nm converge , while they diverge for more than that. This can be easily explained using equations (26,27,31) for large wave lengths where the effects of the impurities manifest themselves through magnetic field, friction, medium potential and natural vibration. The behaviour for small wave lengths can be recognized with the aid of equations (44,48) which reflects absence of the effects of impurities for small wave lengths. Similarly figure (6) for transmittance concerning the same 6 sesame samples indicated considerable change of in the intensity, where the first minimum from the left assume different values which are 10,20, and 37.The second minimum assumes values 10,15 and 30

The UV-VIS spectra shown in figures (6,7,9) concerning sesame ,olive ,nigella sativa ,sun flower and 3 bean oil samples, confirm also the theoretical model. Figure (7) for the absorption against wave length indicated that the curves for the 3 beans samples consisting of different impurities converge for wave lengths less than 240 nm, while they diverge in the range of 270-570nm.In figure (8) the convergence is for less than 240 nm associated with divergence in the range of 340-560 nm. For figure (9) the convergence includes wave lengths less than 240 nm while the divergence is in the range 260-550 nm. The behaviour of the three figures can be explained as in previous discussions utilizing equations (26,27,31,44,48).

5. Conclusion

To see what techniques are suitable for testing oils to determine their purity degree, a nano quantum model based on perturbation theory has been constructed. The theoretical foundations showed that the pure oil spectrum is affected by the medium field potential, friction, internal magnetic field and collision due to free vibration. The wave number and length are affected by the medium field beside free vibration collision, while the intensity is affected by these parameters also in addition to the effects of internal magnetic field and friction, through the exponential term. This means that impurities affects the wave number and length slightly, while it affecting the intensity significantly due to the existence of more parameters beside the enhancing effect of the exponential .These theoretical foundations were confirmed experimentally, where the mixing of pure olive oil with other oils indicated significant effects on the intensity and slight effects on the wave number and length. Such changes increases upon increasing the amount of the mixed oils. The existence of impurities like that observed for bean oil , having different impurities , indicated significant effects on the intensity and slight effects on the wave number and length. The results obtained showed also theoretically and experimentally that the energy of the innermost shells are not affected by the impurities thus assume the same values for all non and contaminated oils .In contrary the energies of the outer most shells are affected by the impurities, thus gives different values .This means that the energies of the outer most shells gives different values for pure and contaminated oils. Hence this indicates that for larger wave numbers and short-wave lengths where the energies are large corresponding to the inner most shells, the

spectral curves for pure and contaminated oils converge and become closer to each other. However, for small wave numbers and longer wave lengths where the energies are small corresponding to the outer most shells, the spectral curves for pure and contaminated oils diverge . Strikingly these theoretical foundations conform with the experimental results obtained for olive and sesame oils

Acknowledgements

The authors thank the deanship in Zarqa University. This research is funded fully by Zarqa University-Jordan.
Conflicts of Interest: The authors declare that they have no conflict of interest.

References

[1] G. Aruldhas, *Quantum Mechanics*, PHI Private Limited, New Delhi, 2009.
[2] D. J. Griffiths, *Introduction to Quantum Mechanics*, Prentice Hall, New Jersey, 2005.
[3] H. Haug and S. W. Koch, *Quantum Theory of the Optical and Electronic Properties of Semiconductors*, 5th ed., World Scientific, Singapore, 2009. https://doi.org/10.1142/7184
[4] P. G. Hewitt, J. A. Suchocki, and L. A. Hewitt, *Conceptual Physical Science*, 5th ed., Pearson, 2011.
[5] S. H. Simon, *The Oxford Solid State Basics*, Oxford University Press, USA, 2013. ISBN 978-0-19-968076-4.
[6] Rohit P. and A. J. Taylor, *Optical Techniques for Solid-State Materials Characterization*, Taylor & Francis Group LLC, New York, 2012.
[7] M. A. Wahab, *Solid State Physics: Structure and Properties of Materials*, Alpha Science, 2005, pp. 1–3. ISBN 978-1-84265-218-3.
[8] L. E. Smart and E. A. Moore, *Solid State Chemistry*, 4th ed., Taylor & Francis Group, Boca Raton, FL, 2016. https://doi.org/10.1201/b12047
[9] R. J. D. Tilley, *Understanding Solids: The Science of Materials*, 3rd ed., Wiley, New York, 2021. ISBN 978-1119716501.
[10] E. L. Wolf, *Nanophysics and Nanotechnology: An Introduction to Modern Concepts in Nanoscience*, 3rd ed., Wiley-VCH, 2015.
[11] G. F. Huseien, N. H. A. Khalid, and Mirza, *Nanotechnology for Smart Concrete*, Taylor & Francis Group LLC, New York, 2022.
[12] S. Shanmugam, *Nanotechnology*, C. Janarthanan, India, 2016. ISBN 978-81-8094-064-4.
[13] K. Huang, *Quantum Field Theory*, Wiley-VCH, Weinheim, 2010.
[14] J. Bunningham and V. Vedral, *Introductory Quantum Physics and Relativity*, Imperial College Press, 2011. ISBN 978-1-84816-514-4.
[15] F. Schmidt, *Laser-based Absorption Spectrometry: Development of NICE-OHMS Towards Ultra-Sensitive Trace Species Detection*, Doctoral dissertation, Fysik, 2007.

[16] J. O. Caceres, S. Moncayo, J. D. Rosales, F. J. M. de Villena, F. C. Alvira, and G. M. Bilmes, Application of Laser-Induced Breakdown Spectroscopy (LIBS) and neural networks to olive oils analysis, *Applied Spectroscopy*, 2013. https://doi.org/10.1366/12-06916

[17] D. Stefas, N. Gyftokostas, E. Nanou, P. Kourelias, and S. Couris, Laser-Induced Breakdown Spectroscopy: An efficient tool for food science and technology, *Molecules* **26** (2021), 4981.

[18] R. M. El-Abassy, P. Donfack, and A. Materny, Visible Raman spectroscopy for the discrimination of olive oils from different vegetable oils and the detection of adulteration, *Journal of Raman Spectroscopy* **40** (2009), 1284–1289.

[19] J. Luo, T. Liu, and Y. Liu, FT-NIR and confocal microscope Raman spectroscopic studies of sesame oil adulteration, *HAL Open Science*, 2016.

[20] B. Lapcikova, T. Valenta, L. Lapcik, and M. Fuksova, Thermal aging of edible oils: Spectrophotometric study, *Potravinarstvo Slovak Journal of Food Sciences* **12**(1) (2018), 372–378.

[21] F. da Silveira Minuceli, J. M. da Silveira, R. da Silveira, and O. Oliveira Santos, UV-Vis spectroscopy methodology for the quantification of vegetable oil in adulterated olive oil, *Research, Society and Development* **10**(6) (2021), e50210612822. http://dx.doi.org/10.33448/rsd-v10i6.12822

[22] N. Vlachos, Y. Skopelitis, M. Psaroudaki, V. Konstantinidou, A. Chatzilazarou, and E. Tegou, Applications of Fourier transform-infrared spectroscopy to edible oils, *Analytica Chimica Acta* **573–574** (2006), 459–465.

[23] A. A. Mudawi and A. A. Marouf, Impact of single wavelength (532 nm) irradiation on the physicochemical properties of sesame oil, *Journal of Materials Science and Chemical Engineering* **10**(4) (2022), 1–15. https://dx.doi.org/10.4236/msce.2022.104001

[24] Y. B. C. Rohman, Authentication of extra virgin olive oil from sesame oil using FTIR spectroscopy and gas chromatography, *International Journal of Food Properties* **15** (2012), 1309–1318.

[25] D.-H. Deng, L. Xu, Z.-H. Ye, H.-F. Cui, C.-B. Cai, and X.-P. Yu, FTIR spectroscopy and chemometric class modeling techniques for authentication of Chinese sesame oil, *Journal of the American Oil Chemists' Society*, 2011. https://doi.org/10.1007/s11746-011-2004-8

[26] A. Menevseoglu, Non-destructive detection of sesame oil adulteration by portable FT-NIR, FT-MIR, and Raman spectrometers combined with chemometrics, *Journal of The Turkish Chemical Society A* **8**(3) (2021), 775–786.

[27] A. A. Bunaciu, D. H. Vu, and H. Y. Aboul-Enein, Detection of sunflower oils adulteration by ATR-FTIR spectra, *Chemical Papers*, 2022. https://doi.org/10.1007/s11696-022-02245-6

[28] S. L. Tan, M. Suhaimy, S. Hanani, and N. A. Abd Samad, Evaluation of fresh palm oil adulteration with recycled cooking oil using GC-MS and ATR-FTIR spectroscopy: A review, *Czech Journal of Food Sciences* **40**(1) (2022).

[29] O. Uncu, B. Ozen, and F. Tokatli, Mid-infrared spectroscopic detection of sunflower oil adulteration with safflower oil, *Grasas y Aceites* **70**(1) (2019), e290.

[30] Y. B. C. Man, Analysis of canola oil in virgin coconut oil using FTIR spectroscopy and chemometrics, *Journal of Food and Pharmaceutical Sciences* **1**(1) (2013).

[31] N. Mashodi *et al.*, Evaluation of extra virgin olive oil adulteration with edible oils using ATR-FTIR spectroscopy, *Malaysian Journal of Applied Sciences* **5**(1) (2020), 35–44.

[32] J. Vilela, L. Coelho, and J. M. M. M. de Almeida, Investigation of adulteration of sunflower oil with thermally deteriorated oil using Fourier transform mid-infrared spectroscopy and chemometrics, *Cogent Food & Agriculture* **1**(1) (2015), 1020254.

[33] S. Syafri, I. Jaswir, F. Yusof, A. Rohman, and D. Hamidi, The use of GC-MS and FTIR spectroscopy coupled with multivariate analysis for the detection of red ginger oil adulteration, *Rasayan Journal of Chemistry* **15**(4) (2022), 2231–2236.

[34] Yousef, M. A. M., M. M. Al-Sawalha, M. A. Al-Saraireh, D. Vranjes, and B. Wehbe. 2022. "Electronic Chips Acting as Capacitors or Inductors When Laser Acts as Information Transmitter." East European Journal of Physics (2): 141–152. https://doi.org/10.26565/2312-4334-2022-2-18.

[35] M. A. Allam and S. F. Hamed, Application of FTIR spectroscopy in the assessment of olive oil adulteration, *Journal of Applied Sciences Research* **3**(2) (2005), 102–108.

[36] M. U. Orsod, M. D. Abdalla, G. Krishnan, B. O. Elbashir, and F. M. B. Elshafia, Identification of Sudanese sesame oil quality using a 680 nm semiconductor laser spectrometer and other techniques, *Optics and Photonics Journal* **14** (2024), 29–45.